RSC Advances

PAPER

View Article Online
View Journal | View Issue

Cite this: *RSC Adv.*, 2016, **6**, 49633

Study on thermal degradation and combustion behavior of flame retardant unsaturated polyester resin modified with a reactive phosphorus containing monomer

Ying Lin,[a] Bin Yu,[ab] Xin Jin,[a] Lei Song*[a] and Yuan Hu*[ab]

A halogen-free phosphorus-containing monomer (TAOPO) with a P–C bond was successfully synthesized and used as a co-curing agent to prepare intrinsic flame-retardant unsaturated polyester resin (FR-UPR) by radical bulk polymerization with different TAOPO content. The thermal degradation and flame retardancy of pure UPR and FR-UPR were investigated by thermogravimetric analysis (TGA), cone calorimetry tests and limiting oxygen index (LOI). As the phosphorus content increased to 3%, FR-UPR (URP-3) showed a lower peak heat release rate (PHRR) and total heat release (THR), reducing by 45.7% and 45.5% those of pure UPR, while the LOI value and char residue increased markedly. Besides, thermal-oxidative degradation behaviors of different UPR samples were characterized by real-time infrared spectrometry (RT-IR) and thermogravimetry-Fourier transform infrared (TG-FTIR) spectroscopy, revealing the degradation mechanism. Furthermore, the residual char of UPRs was investigated by scanning electron microscopy (SEM) and Raman spectroscopy. The results indicated that the incorporation of TAOPO into UPR could effectively prompt the UP matrix to form a more compact char layer which acted as a protective barrier to reduce heat release during combustion.

Received 11th March 2016
Accepted 12th May 2016

DOI: 10.1039/c6ra06544a

www.rsc.org/advances

1. Introduction

Unsaturated polyester resin (UPR), as an important thermoset material, has been widely used in the field of coatings, transportation and building construction due to its comparatively low price, easy processing and excellent mechanical properties as well as good comprehensive performance after curing.[1–3] However, conventional UPR is susceptible to high temperature and behaves poorly under fire conditions (*e.g.*, highly flammable and produces a large amount of smoke and toxic gases when combusted) because of the intrinsic chemical composition and molecular structure, which seriously limits its further application in some areas.[4,5]

To overcome the aforementioned drawbacks of UPR, many approaches have been adopted to improve its thermal stability and flame retardant properties. There are generally two effective ways. One is additive-type flame-retarded modification that is to blend the non-reactive additives and UPR matrixes; the other is intrinsic flame-retarded modification—to introduce reactive flame retardant monomers into UP chain or prepolymer, and they undergo cross-link copolymerization under appropriate conditions.[6] The incorporation of reactive monomers into polymeric structure is recognized as a more efficient way to obtain an excellent flame retardant polymer system than the former. Reactive monomers can markedly enhance the fire-resistance efficiency of some polymer materials even at low dosage, which also has little side effects to mechanical properties of polymer matrixes.[2,7–9]

In the recent decades, phosphorus-containing flame retardants, such as phosphine oxides, phosphonium compounds, phosphonates, phosphites and phosphate, have been extensively studied as promising substitutes for the halogenated compounds.[10] The presence of which plays a significant role in the high performances of fire-retarded polymers due to its ability to inhibit ignition and promote char formation during plastic matrix decomposition.[11] Also, some phosphorus-containing compounds or co-monomers can effectively improve flame retardant properties and thermal stabilities of unsaturated polyester resin. Ammonium polyphosphate (APP), as an intumescent flame retardant, can lead to a significant influence on thermal stability and flame retardant property of UPR by promoting the formation of high quality char during thermal degradation.[12,13] Chen *et al.*[6] reported a reactive flame retardant UPR from a phosphorus-containing diacid (DDP), which showed good thermal stability and higher LOI value

[a]*State Key Laboratory of Fire Science, University of Science and Technology of China, 96 Jinzhai Road, Hefei, Anhui 230026, P. R. China. E-mail: leisong@ustc.edu.cn; yuanhu@ustc.edu.cn; Fax: +86-551-63600081; +86-551-63601664; Tel: +86-551-63600081; +86-551-63601664*

[b]*USTC-CityU Joint Advanced Research Centre, Suzhou Key Laboratory of Urban Public Safety, Suzhou Institute for Advanced Study, University of Science and Technology of China, 166 Ren'ai Road, Suzhou, Jiangsu 215123, P. R. China*

(~29), and reached V-0 rating in UL-94 test when 18.1 wt% DDP was incorporated. Kang *et al.*[14] synthesized a cyclic reactive monomer with high phosphorus content (EACGP) that had reduced the mass loss rate and improved the char yield of UPR when incorporated into matrix. Meanwhile, EACGP had obvious effects on decreasing peak heat release rate (PHRR) and total heat release (THR) of UPR. In addition, based on the previously published literatures, phosphine oxides containing P–C bond are more stable than the compounds that only contain P–O–C bond among these phosphorus-containing flame retardants.[15–18] The former possess higher thermal stability and resistance to moisture, on account of better anti-hydrolysis ability of P–C bond. Therefore, it can be an effective way to improve the flame retardant property of polymers by incorporating chemical units containing phosphine oxides with P–C bond into polymer matrixes. Although, some of phosphine oxides have been used as effective flame retardant for several polymer matrixes, such as epoxy resin,[17,18] little attempt was made to incorporate reactive phosphine oxide monomers with P–C bond into unsaturated polyester resins.

In this work, a flame retardant phosphine oxide monomer with P–C bond was synthesized, and then copolymerized with unsaturated bonds of UP in different ratios to obtain a flame-retardant unsaturated polyester resin with excellent comprehensive performance. The fire safety property, thermal degradation and fire-retardant mechanism were investigated.

2. Experimental

2.1 Materials

Orthophthalic unsaturated polyester (196# type, commercial grade) was obtained from Hefei Chaoyu Chemical Co., Ltd. (Anhui, China). Tetrakis (hydroxymethyl) phosphonium sulfate (THPS, 75% solution) was supplied by Aladdin Industrial Inc. (Shanghai, China); Allyl chloride (CP) was provided by Xiya Chemical Industries Co., Ltd. (Sichuan, China); barium hydroxide (CP), hydrogen peroxide (30%, AR), sodium hydroxide (AR), chloroform (AR), anhydrous sodium sulfate (AR), catalyst benzyltriethylammonium chloride (CP) and initiator benzoyl peroxide (BPO, CP) were purchased from Sinopharm Chemical Reagent Co., Ltd. (Shanghai, China). BPO was purified by recrystallization from chloroform and methanol before use. Other reagents were used as received.

2.2 Synthetic procedures

Synthesis of Tris (hydroxymethyl) phosphine oxide (THPO). THPO was synthesized based on the previously published literatures.[19] The synthetic route is shown in Scheme 1.

Synthesis of Tris (allyloxymethyl) phosphine oxide (TAOPO). TAOPO was synthesized according to the method described in the previous report.[20,21] A three-necked round-bottom flask equipped with magnetic stirrer, an additional funnel, a circumference condenser and thermometer was employed. To begin, benzyl-triethylammonium chloride (10% weight of THPO) was well dissolved in THPO (0.1 mol) with stirring. Then sodium hydroxide aqueous solution (30%) was added slowly, maintaining the reaction temperature below 35 °C. After that, the mixture was cooled to 0 °C in an ice bath. Next, allyl chloride (0.36 mol) was added by dropwise into the flask with stirring for 2 hours at low temperatures (<5 °C). Subsequently, the system temperature was increased to 45 °C, maintaining for 10 hours, then cooled to ambient temperature. Following this, crude product was washed with a large amount of distilled water for several times until chloride ion was completely undetectable by Ba^{2+}, and dried with anhydrous Na_2SO_4. After filtration, the excess reactants were removed by atmospheric distillation at 45 °C. Finally, the remaining product was dried under vacuum overnight. The detailed synthetic route is illustrated in Scheme 1. Yield: 75%. ^{1}H NMR (400 MHz, DMSO-d_6), δ: 4.07 ppm (6H, P–CH_2–O), 3.86 ppm (6H, O–CH_2–C), 5.87 ppm (3H, –CH=), 5.18–5.31 ppm (6H, =CH_2). ^{31}P NMR (400 MHz, DMSO-d_6), δ: 37.56 ppm (1P, O=P–C). FTIR (KBr): 3081.7 (=C–H), 2982.9 and 2857.1 (–CH_2), 1645.3 (C=C), 1180.1 (P=O), 1090.4 (C–O–C).

2.3 Preparation of flame retardant UPR/TAOPO samples

Different amount of reactive monomer (TAOPO) was added into UPR (according to the control of phosphorus content in UPR, listed in Table 1) at room temperature with vigorous agitation for about half an hour. Then radical initiator BPO (2 wt%) was applied in homogeneous viscous liquid obtained in last step, stirring for another 20 minutes. After the removal of air bubbles in the mixture through the method of vacuum, casting composition was rapidly poured into Teflon mold, pre-cured at 70 °C for 3 h, post-cured at 120 °C for 2 h. Finally, samples were cooled slowly to room temperature. The curing process was shown in Fig. 1.

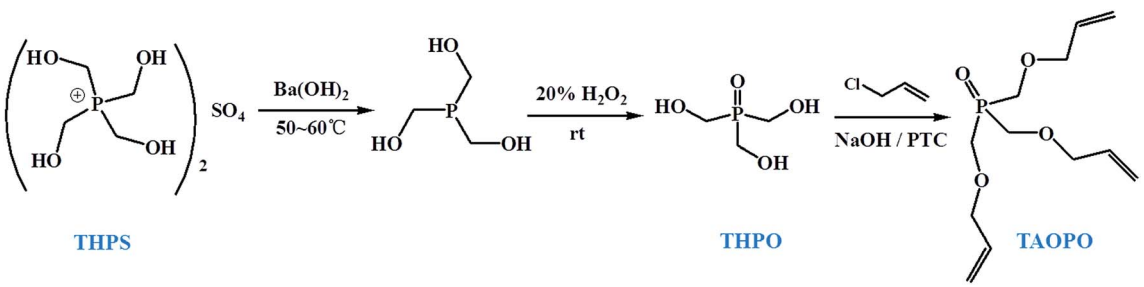

Scheme 1 The synthetic routes of THPO and TAOPO.

Table 1 Formulations and appearance of UPR and UPR/TAOPO samples after curing

Sample	UPR content (%)	TAOPO content (%)	Phosphorus content (%)	BPO content[a] (UPR %)	Appearance of UPRs
UPR	100	0	0	2.0	Transparent
UPR-1	91.6	8.4	1.0	2.0	Transparent
UPR-2	83.2	16.8	2.0	2.0	Light yellow
UPR-3	74.5	25.5	3.0	2.0	Light yellow

[a] BPO content is based on the weight percent of UPR.

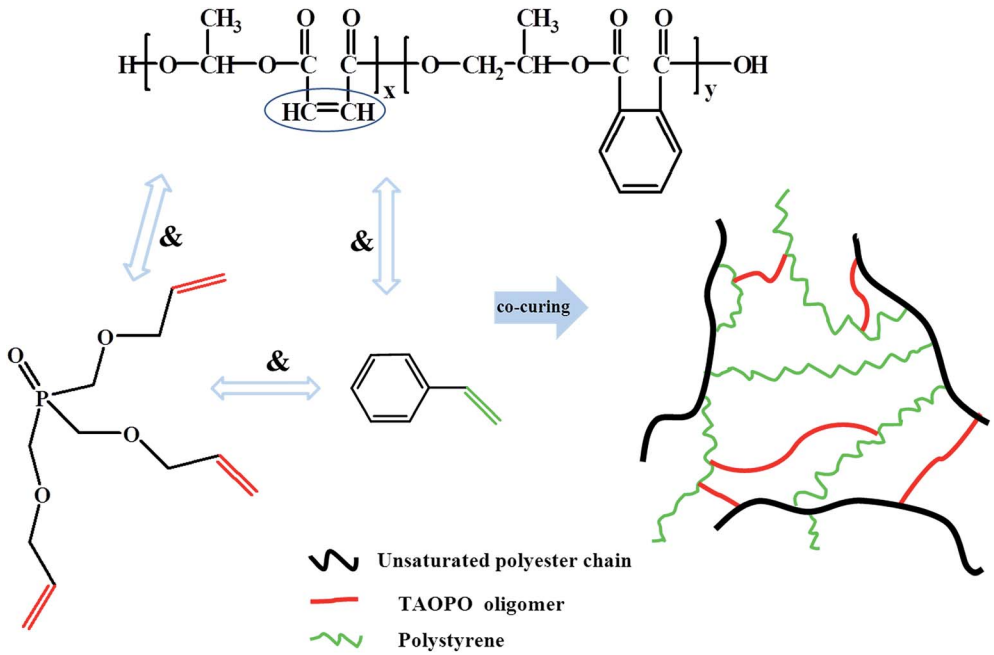

Fig. 1 The curing process of flame retardant UPR samples.

2.4 Measurements

Thermogravimetric analysis (TGA) was carried out on a Q5000 IR thermogravimetric analyzer (TA instruments), heating from ambient temperature to 700 °C at a rate of 20 °C min^{-1} in air and nitrogen atmosphere, respectively. The weight of each sample was about 3–10 mg.

Thermogravimetry-Fourier transform infrared (TG-FTIR) spectroscopy was for analyzing evolved gas of pyrolysis. It was performed on the TGA Q5000 IR thermogravimetric analyzer that was interfaced to the Nicolet 6700 FTIR spectrophotometer. The samples were heated from room temperature to 700 °C with the heating rate of 20°C min^{-1} under N_2 condition during the test.

Real-time infrared spectroscopy (RTIR) was carried out using a Nicolet MAGNA-IR 750 spectrophotometer equipped with a heating device and temperature control apparatus. The powdery samples were mixed with KBr, then pressed into a tablet, following by placing them in a ventilated oven, heating at a rate of 10°C min^{-1} during the test.

Limiting oxygen index (LOI) measurement was carried out at room temperature on a HC-2 LOI meter according to standard ASTM D2863. And the sample dimensions were 100 × 6.5 × 3 mm^3.

The combustion behaviors of the samples (dimensions: 100 × 100 × 3 mm^3) were investigated by a cone calorimeter (Fire Testing Technology, UK) according to ISO 5660 standard. Each specimen was wrapped in an aluminum foil and only the upper surface was exposed horizontally to 35 kW m^{-2} external heat flux.

Scanning electron microscopy (SEM) was used to investigate the morphology of the char residue on a scanning electron microscope AMRAY1000B. The specimens were previously coated with a conductive gold layer.

Raman spectroscopy (RS) measurements were performed at room temperature using a SPEX-1403 laser Raman spectrometer (SPEX Co, USA) with excitation provided in back-scattering geometry by a 514.5 nm argon laser line.

3. Results and discussion

3.1 Thermal degradation analysis

The thermal stability and degradation behaviors of flame retardant unsaturated polyester (FR-UPR) and pure sample were investigated by thermogravimetric analysis (TGA) under both

air and nitrogen condition. Fig. 2 and 3 illustrate the TGA and differential thermogravimetry (DTG) curves of polymer material samples in air and N_2 atmosphere, respectively. And the relative details are listed in Table 2. In addition, the initial degradation temperature (T_d) is considered as the temperature at 5% weight loss, and T_{max}, defined as the temperature at the maximum weight loss rate, was found in the DTG curves. And the yield of residual char at 600 °C was obtained from TGA curves. It can be found from the TGA curves (Fig. 2(a)) that thermal oxidative degradation process of polymer samples consisted of three stages. The initial degradation step was in the temperature range of 200–330 °C, resulting from mass loss of water dehydration. While the second degradation stage, occurring at 300–420 °C, could be ascribed to chain scission of polymer fragments (involving polystyrene and polyester), corresponding to a strong peak in DTG curves at around 395 °C. This thermal degradation process led to the formation of a metastable carbonaceous char which can be degraded further at higher temperature regions above 550 °C in the third stage, and in this last step, as the TAOPO content raised, the char residue left increased markedly (Table 2). Specifically, the char yield of sample without TAOPO only remained 0.68 wt% at 600 °C, while that of UPR-3 reached to 8.01 wt%, indicating the phosphorus containing monomer can be effective to promote char-formation of UPR matrices.

However, under nitrogen condition, the degradation behaviors of all samples were significantly different from those in air. As shown in Fig. 3(a), the thermal degradation process of each sample consisted of two stages. The first step, occurring at 200–320 °C, was ascribed to water elimination reaction and the decomposition of TAOPO. Meanwhile, compared T_d for UPRs at ~250 °C, FR-UPRs degraded earlier than neat resin in lower temperature. It could be due to the decomposition of relatively weak chemical bond P–C–O in TAOPO molecular at lower temperature, which was consistent well with the pyrolysis behavior of phosphorus-based flame retardants reported previously.[5,22] Moreover, T_{max} of FR-UPRs was slightly higher than that of pristine resin with relatively lower maximum mass loss rate, suggesting the UPR with TAOPO degraded more slowly and possessed higher thermal stability. Besides, the third degradation process in air atmosphere disappeared under nitrogen condition, and the char residue of all samples increased slightly than those in air, suggesting that oxygen could facilitate the degradation of polymer materials. Also, it is clear that the char yield at 600 °C for pure sample and UPR-3 was 7.84% and 10.74%, respectively. And the char residue of flame retardant samples improved obviously with the TAOPO content increased, demonstrating the residual char of UPR containing TAOPO was more stable in high temperature (>500 °C), which was similar to the results under air in Table 2.

The TGA and DTG results revealed that chemically incorporating flame retardant monomer with UPR could affect the degradation behavior of resin matrix. Although the initial decomposition temperature of FR-UPR declined slightly, the thermal stability and char yield improved at relatively higher temperature region, indicating that the phosphine oxide might play a positive role in promoting charring because of the formation of phosphoric acid during pyrolysis. Furthermore, this phosphorated residual char exhibited high thermal stability, and acted as a barrier to prevent heat and combustible gases transferring, thus protecting underlying materials.

3.2 TG-FTIR analysis on evolved gas of pyrolysis

In order to explore the primary thermal degradation mechanism in gas phase of UPRs, a further study on gaseous pyrolysis products of UPR and FR-UPR during combustion was carried out by TG-IR technique which could significantly identified the various gaseous products from decomposition. Fig. 4(a) and 5(a) show the FTIR spectra of evolved gas products from pyrolysis of UPR and UPR-3 at the maximum mass loss rate (MMLR), respectively. And the relative DTG curves were presented in (b) (Fig. 4 and 5). Fig. 6 depicted the differences in TG-IR spectra of gaseous products during thermal degradation at MMLR of pure UPR and UPR-3. Comparing those figures (Fig. 4(a), 5(a) (curve 1) and 6), it is clear that no obvious differences in pyrolysis product species between two samples except some weak absorbances at 1170 cm^{-1}, 1488 cm^{-1} and 775 cm^{-1} that may be attributed to compounds containing phosphorus (corresponding to functional groups of P═O and P–C), indicating the introduction of TAOPO had little effect on the main species of evolved gas during pyrolysis. Meanwhile, the gaseous small

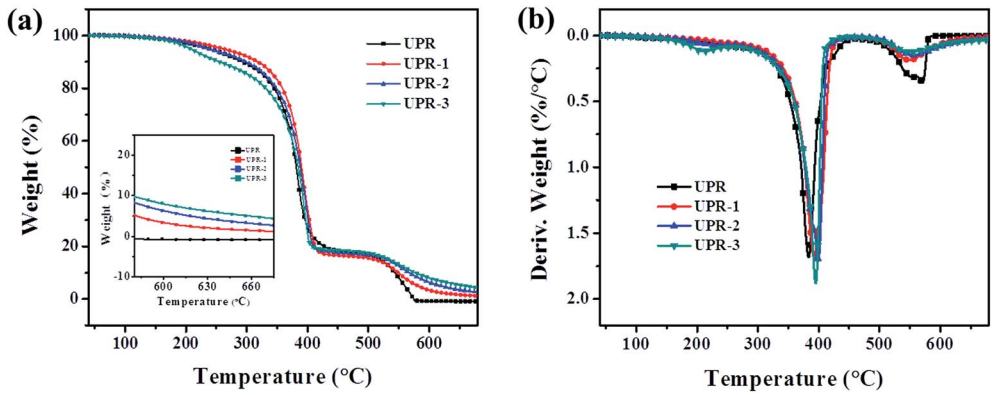

Fig. 2 (a) TGA and (b) DTG curves of different UPR samples in air atmosphere.

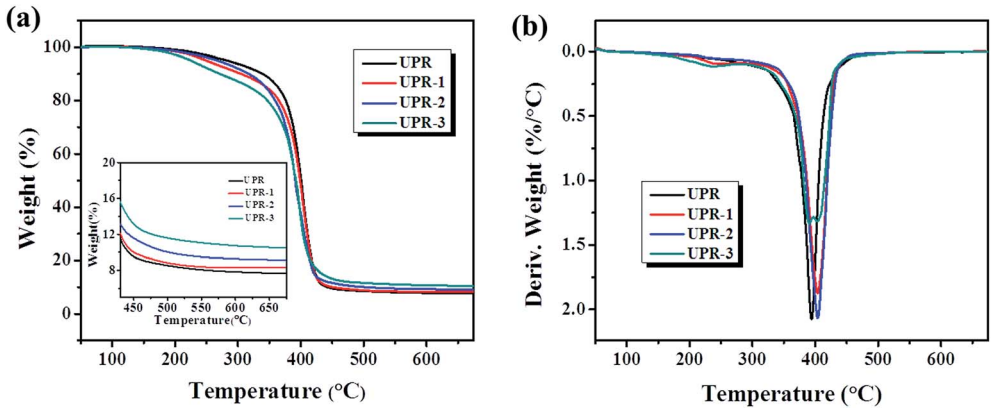

Fig. 3 (a) TGA and (b) DTG curves of different UPR samples in N_2 atmosphere.

Table 2 TGA data of UPR and flame retardant UPR in air and nitrogen atmosphere

		T_d (°C)		T_{max} (°C)		Char (600 °C, wt%)	
Sample	P content (wt%)	Air	N_2	Air	N_2	Air	N_2
UPR	0	238	283	383	394	0.68	7.84
UPR-1	1	259	250	392	403	3.38	8.31
UPR-2	2	236	268	398	404	6.33	9.28
UPR-3	3	206	225	397	396	8.01	10.74

molecules can be easily identified by the characteristic peaks in the infrared region. Specifically, the signals at around 3550–3800 cm^{-1}, 3150–2800 cm^{-1}, 2400–2200 cm^{-1}, 1900–1650 cm^{-1} and 1500–600 cm^{-1} fitted well to the reported FTIR features of volatile products such as H_2O (3500–3800 cm^{-1}), hydrocarbons (2950–2850 cm^{-1}), CO_2 (2400–2300 cm^{-1}), CO (2300–2200 cm^{-1}), anhydride (1900–1840 cm^{-1}) and carbonyl compounds (1800–1700 cm^{-1}).[23,24]

On the other hand, compared with the DTG data in Fig. 4(b) and 5(b), two peaks appeared in the DTG curves at around 220 °C and 380 °C of UPR-3, and only one absorption signal at 390 °C can be observed in DTG curve of pure UPR, indicating that thermal degradation process of UPR-3 consisted of two stages, while that of neat UPR presented only one. In addition, the FTIR spectra of gaseous products at the first degradation stage of UPR-3 (see Fig. 5(a) curve 1) exhibited several characteristic absorption at 1480 cm^{-1} and 800 cm^{-1}, suggesting the gas phase was mixed with phosphorus containing compound. Therefore, considering the similar structure of two samples, the results above revealed that the preceding degradation step of flame retardant UPR is mainly about the decomposition of TAOPO oligomer, which demonstrated the flame retardant mechanism based on gas phase may occur as expected.

Fig. 7 illustrates the selected FTIR spectra of some volatilized products (hydrocarbons, CO_2, anhydride and carbonyl compound) from pyrolysis of UPR and UPR-3 at MMLR, respectively. It is obvious that the UPR with TAOPO shows much lower absorbance intensity than that of pristine sample. It may

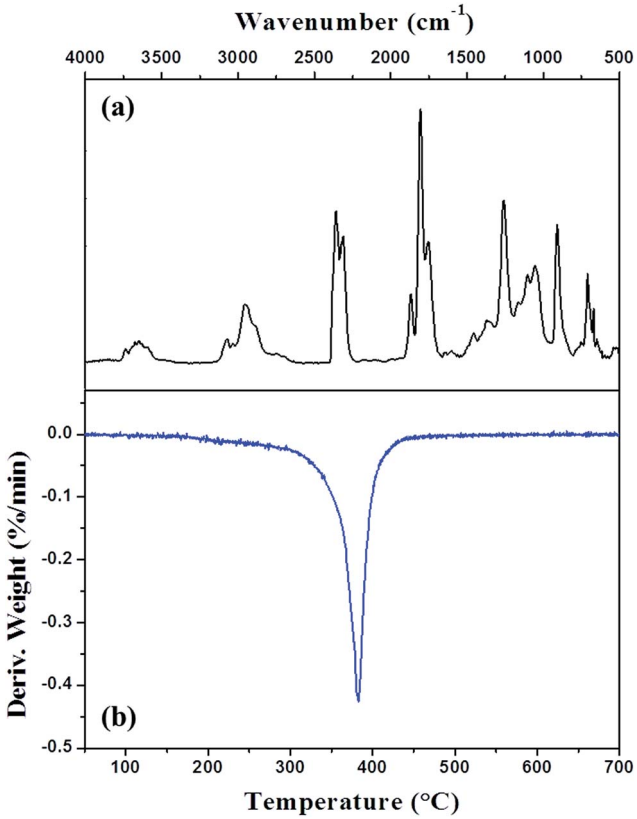

Fig. 4 (a) FTIR spectrum of pyrolysis products for UPR at the maximum degradation rate and (b) corresponding DTG curve.

be caused by the reaction of TAOPO oligomer (& matrix) in UPR-3 during degradation, which led to decrease in gaseous products intensity. Also, a large amount of char layer formed in the period of decomposition acted as a barrier to minimize the evolved gas and heat release. Moreover, the maximum degradation rate signals of volatile products for UPR-3 came earlier than UPR, indicating that the flame retardant UPR degraded earlier, which accorded well with the TG results. Consequently, the incorporation of TAOPO into UPR could improve the flame retardant property based on gas phase.

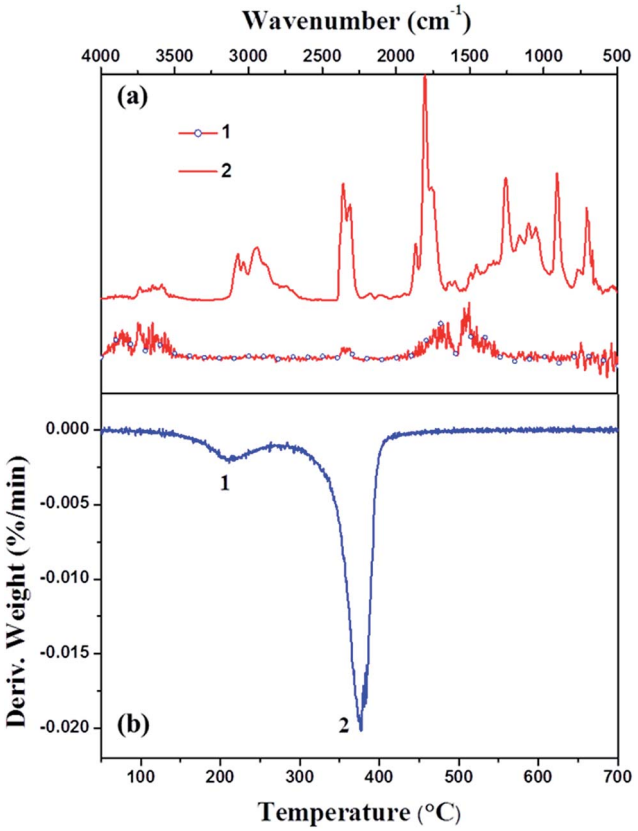

Fig. 5 (a) FTIR spectra of pyrolysis products for UPR-3 at the maximum degradation rate and (b) corresponding DTG curve.

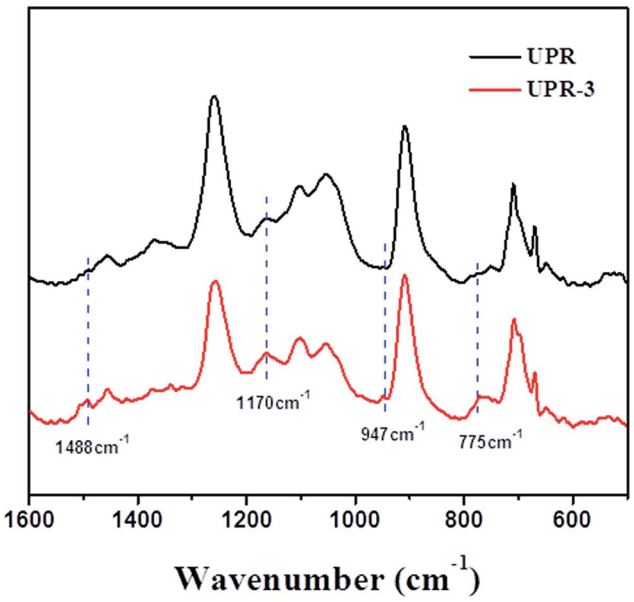

Fig. 6 TG-IR spectra of pyrolysis products at maximum degradation rate of UPR and UPR-3 (comparison diagram).

3.3 RT-IR analysis on condensed product of pyrolysis

The real time infrared spectra (RT-IR) are employed to investigate the different thermal-oxidative degradation behaviors of UPRs before and after incorporation of TAOPO *via* analyzing the solid-state pyrolysis products of them. Fig. 8 reveals the RT-IR spectra of neat UPR and UPR-3. As shown in Fig. 8(a), the characteristic absorptions of pure UPR are listed as follows: 3490 cm^{-1}, stretching vibration of –OH; 2957 cm^{-1}, asymmetrical stretching vibration of $-CH_2$; 1732 cm^{-1} and 1272 cm^{-1} & 1148 cm^{-1}, ester group (stretching of C=O and symmetrical stretching of C–O–C, respectively);[25] 1448 cm^{-1}, 747 cm^{-1} and 696 cm^{-1}, aromatic ring. And all these absorption peaks were obvious at ambient temperature. But as the temperature rose, some alterations appeared. Particularly, the relative intensity of peak at 3490 cm^{-1} declined significantly at 250–300 °C, and completely vanished at 350 °C, which ascribed to the evolution of H_2O and the loss of hydroxyl groups. Besides, only little variation can be observed when temperature below 350 °C for other characteristic peaks. However, with the temperature increasing further, the intensity of all absorption bands reduced drastically, indicating that the main thermal-oxidative degradation of unsaturated polyester and polystyrene chains happened in the temperature range of 350–420 °C. What's more, all peaks almost disappeared when the temperature reached 420 °C, suggesting that the UPR degraded totally.[26] All results above are consistent well with TGA results.[27]

Compared to the pure UPR, UPR-3 showed somewhat different in the degradation behavior at relatively higher temperature. And the RTIR spectra of UPR-3 are given in Fig. 5(b). Although most characteristic absorption peaks can be found in the spectrum at ambient temperature, the absorption of P=O (1280 cm^{-1}) and P–C (1480 cm^{-1}) were difficult to discriminate clearly, because they overlapped with the C–O–C stretching vibration peak and aromatic absorption band, respectively.[28] Whereas the absorption peaks at 1280 cm^{-1}, 1083 cm^{-1}, 880 cm^{-1} still exist in a higher temperature above 420 °C, which differed from those of pure UPR. These peaks could be assigned to asymmetric stretching vibration of P–O–P.[29] This demonstrated that phosphine oxide had poor heat resistance and transformed into more stable polyphosphates at higher temperature.[30] Meanwhile, the absorption bands at 748 cm^{-1} and 699 cm^{-1} indicated the formation of aromatic residue char during the pyrolysis in high temperature zone (>420 °C). And the compact char layer could prevent the further degradation of polymer matrix in the combustion.

3.4 Flame retardant and combustion behavior analysis

Limiting oxygen index (LOI) is defined as the minimum volume percentage of oxygen in a mixture which consists of oxygen and nitrogen to just support the combustion of sample strip.[31] This parameter is used to evaluate the flammability of material. The results of LOI test for flame retardant unsaturated polyester and pure samples are presented in Table 3. The UPR without TAOPO showed a low LOI value at 20.5%, whereas the flame-retardant UPRs exhibited a higher LOI value which arose with the increasing mass fraction of TAOPO. When the phosphorus content of the flame retarded polymer sample (UPR-3) enhanced to 3 wt%, its LOI value reached up to 27%. The

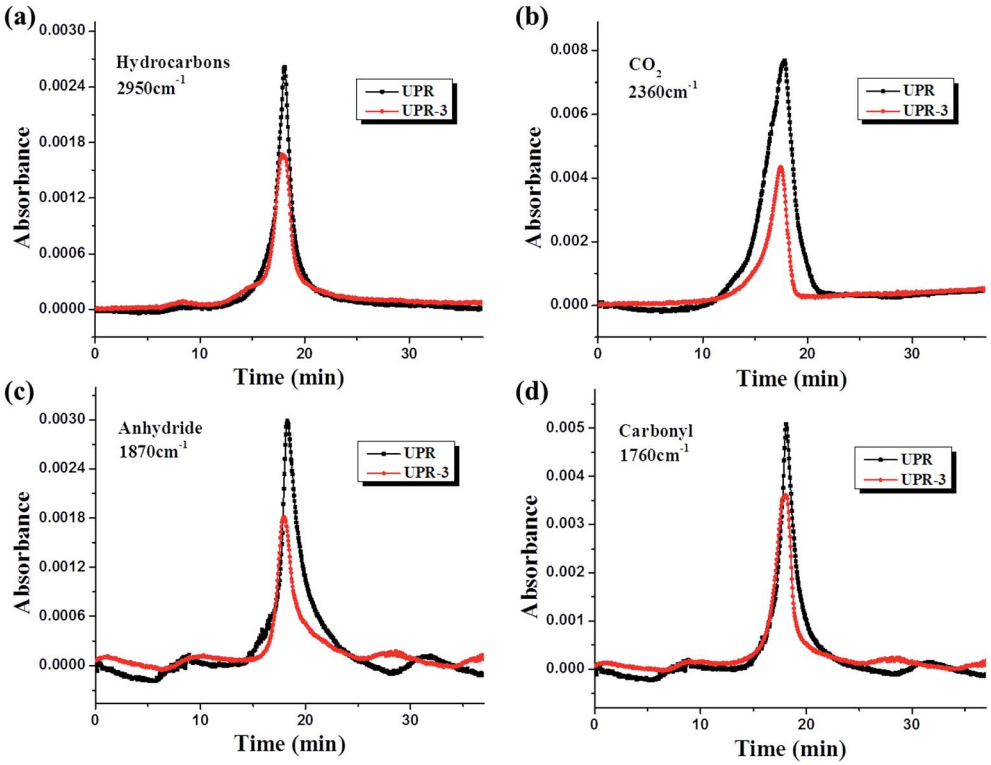

Fig. 7 TG-FTIR spectra of (a) hydrocarbons, (b) CO_2, (c) anhydride and (d) carbonyl compound at the maximum degradation rate for UPR and UPR-3.

results demonstrated that the reactive monomer showed certain flame retardant effect on UPRs.

Cone calorimeter test is widely applied to investigate the combustion behavior of polymeric materials.[32] From which, the statistics of heat release rate (HRR) and total heat release (THR) can be obtained. The curves of those are shown in Fig. 9. And the relative data is given in Table 3. It is clear that the incorporation of TAOPO into UPR had a significant effect on combustion behavior of polymer samples. With the introduction of flame retardant, the peak heat release rate (PHRR) and THR of UPRs decreased markedly. Specifically, the neat sample

Table 3 LOI values and cone data (PHRR and THR) of UPR and FR-UPR

Sample	LOI (%)	PHRR (kW m^{-2})	THR (MJ m^{-2})
UPR	20.5	849	49.9
UPR-1	25	585	37.7
UPR-2	26	547	34.9
UPR-3	27	461	27.2

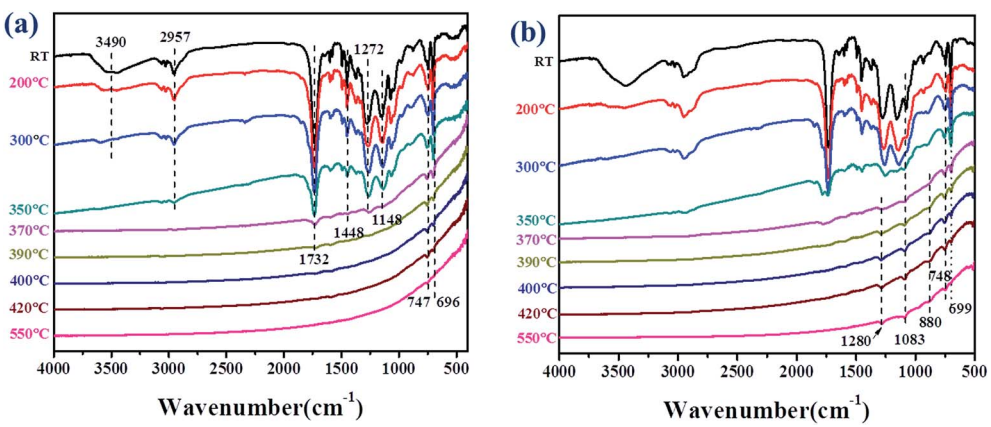

Fig. 8 FTIR spectra of (a) UPR and (b) UPR-3 at different temperatures.

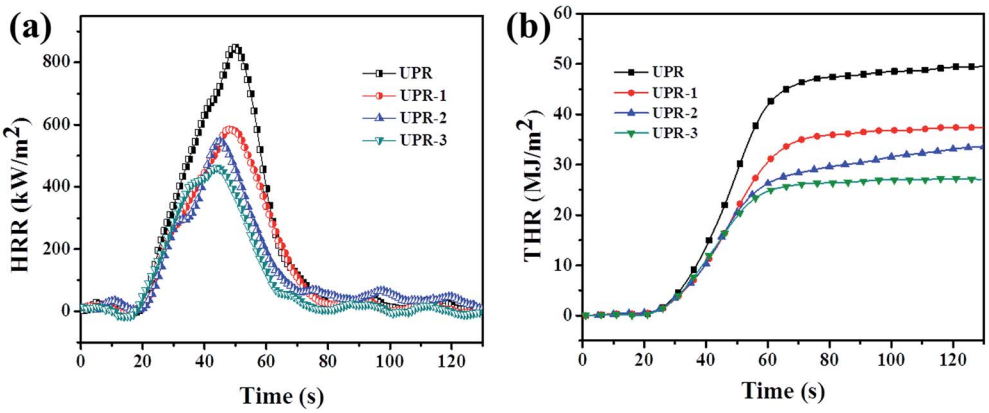

Fig. 9 (a) HRR and (b) THR curves of UPR and FR-UPR samples under a 35 kW m^{-2} heat flux.

presented a rapid combustion with high PHRR (849 kW m^{-2}) and THR (49.9 MJ m^{-2}) values (see Table 3), and remained only a small amount of char residues after the test (Fig. 10). Unlikely, when TAOPO was incorporated to UPR with 3 wt% phosphorus content, a much lower PHRR (461 kW m^{-2}) and THR (27.2 MJ m^{-2}) can be observed, having fallen by about 45.7% and 45.5% than those of pure UPR, respectively. Meanwhile, UPR-3 possessed the most char yield of all after burning, which accorded with TGA results. Besides, when the phosphorus content of fire retardant polymer samples increased from 0 to 2 wt%, PHRR and THR values of UPR-1 drop to 585 kW m^{-2} and 37.5 MJ m^{-2}, respectively. While those of UPR-2 show relatively lower (547 kW m^{-2}, 34.9 MJ m^{-2}), indicating that TAOPO can promote UPR matrix to form a protective char layer and decline heat release during combustion effectively.

Besides, the smoke release property is also considered as a valuation on fire safety of polymer materials.[33] Conventional UPR is highly flammable and produces a large amount of smoke during combustion, mainly due to styrene component and some other aromatic structures.[30] Although phosphorus-containing flame retardants can significantly improve the flame-retarded property of UPR, they are not all effective in reducing smoke emission. Furthermore, some phosphorus-containing monomers and compounds with aromatic structures may raise the smoke emission rapidly as the increase of adding amount,[6] attributed to aromatic structures that produce more smoke when burning. Moreover, layered double hydroxides and some metal compounds can be as smoke suppressing agents for UPR.[27,34,35]

3.5 The characterization of residual char

The compact carbonaceous char, constructing during burning process, is a protective barrier which acts as a thermal insulation layer to prevent matrix pyrolysis and inhibit the transfer of flammable gases and heat between both gas and condensed phases during combustion.[36] Therefore, the morphology of residual char is of great value in evaluating the flame retardancy of materials.[37] And the residues were obtained from pyrolysis of polymer samples in a muffle furnace at 600 °C for 10 minutes. Fig. 11 shows SEM images of the outer char residue of pure UPR and TAOPO/UPR samples. As shown in Fig. 11(a), many holes and pits can be observed on the char surface, which may serve limited insulation effect. On the contrary, the image of UPR-3 char exhibited a much more compact and smooth surface with

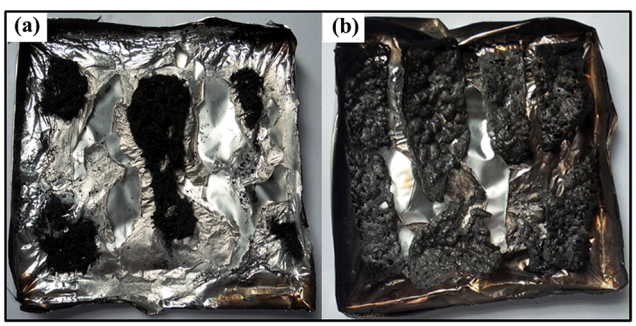

Fig. 10 Photos of (a) UPR and (b) UPR-3 after the cone calorimetry test.

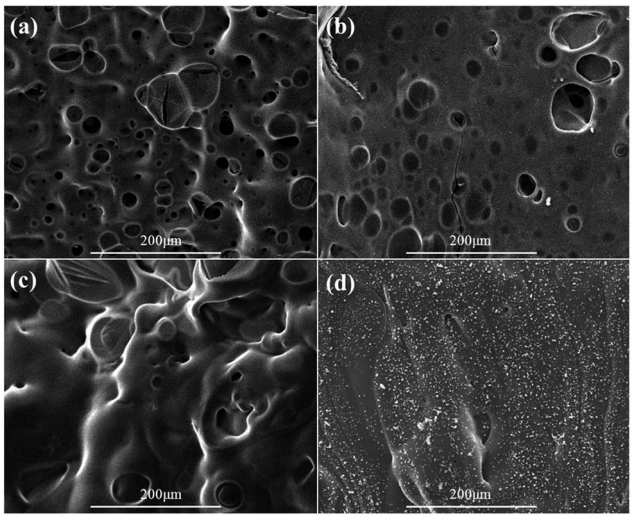

Fig. 11 SEM images of the outer char residue of (a) UPR, (b) UPR-1, (c) UPR-2 and (d) UPR-3.

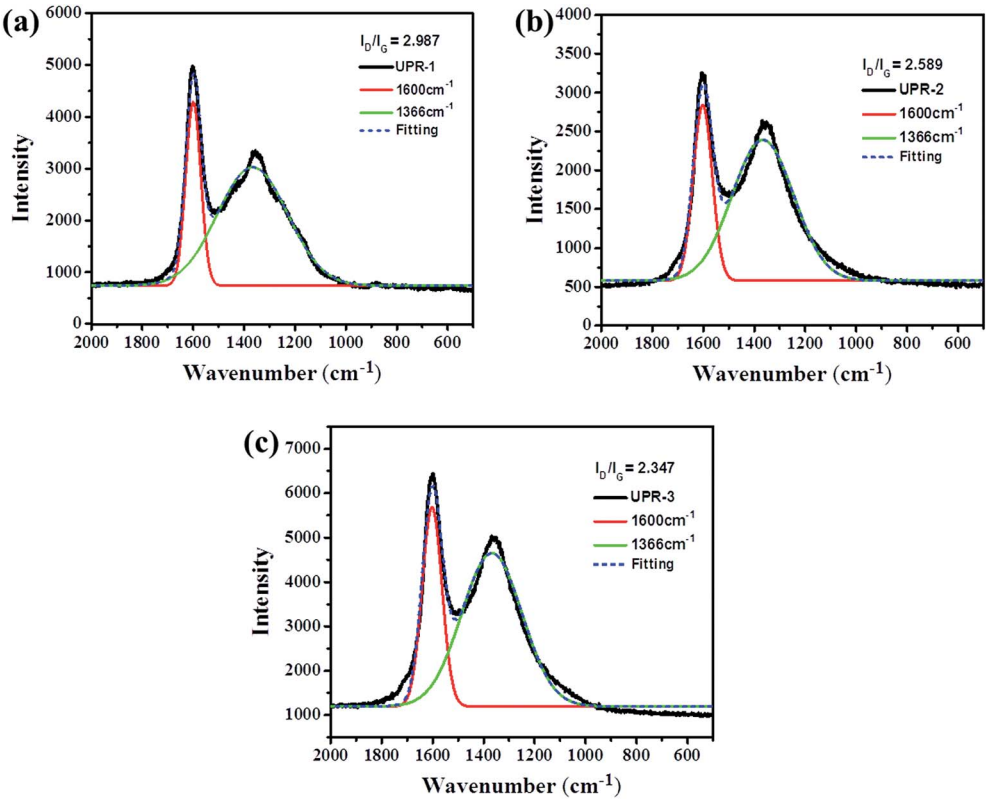

Fig. 12 Raman spectra of char residues for FR-UPR samples.

only few pores (see Fig. 11(d)), which could play an effective part on heat barrier. Besides, fewer holes on the char surface can be observed with the increase of TAOPO content on flame retardant UPRs (Fig. 11). As a result, it indicated that the flame retardant component can promote the polymer matrix to construct a protective char layer on the surface during pyrolysis and combustion, reducing the production of combustible volatiles.

Raman spectroscopy is used to evaluate the structural order degree of carbonaceous char layer. And two characteristic bands appear on the spectra: D and G bands, at ~1366 cm^{-1} and 1600 cm^{-1}, which are typical of disorganized carbon and graphitic phases, respectively.[38,39] According to the reports previously, the relative intensity ratio of two bands (I_D/I_G) can reflect the graphitization degree of carbon materials.[40,41] Fig. 12 shows the Raman spectrum which was dealt with peak fitting to obtain 2 Gauss bands of each flame retardant UPR sample. Generally, the increasing of the I_D/I_G ratio can indicate a decrease of graphitization degree in char layer.[42] It can be seen that (in Fig. 12) the I_D/I_G ratios of three flame retardant UPR, in decrease order, were UPR-1(2.987) > UPR-2(2.589) > UPR-3(2.347), suggesting char layer of UPR-3 possessed the highest graphitization degree and the best performance in char forming, which can be employed to explain its highest char yield in TGA test under air and N_2 atmosphere. Moreover, the I_D/I_G ratio of UPR-2 was lower than that of UPR-1, corresponding to the TGA results that more char residue left for UPR-2 after pyrolysis. Raman results were consistent well with TGA data in both air and nitrogen environment.

4. Conclusions

In this work, a reactive flame retardant phosphine oxide monomer with P–C bond (TAOPO) was successfully synthesized. TAOPO copolymerized with unsaturated polyester in different ratios, resulting in flame-retardant UPRs with excellent comprehensive performance. All the test results of flame-retarded UPR indicated high temperature thermal stability, combustion property and flame retardancy of TAOPO/UPR have improved greatly. TGA data revealed that TAOPO can strengthen the thermal stability of UPR matrix and produced additional carbonaceous residue in higher temperature region. PHRR and THR value of UPR-3 from cone calorimetry experiments reduced significantly, corresponding to the increase of LOI value. The flame retardant mechanism was investigated by TG-FTIR and RT-IR spectroscopy, indicating that the phosphine oxide oligomer in flame retardant UPR can decline the release of volatile gas during pyrolysis and transformed into more thermally stable polyphosphates species at higher temperature, giving rise to highly structured char residue which prevented the further degradation of the underlying polymer matrix, fully according with SEM results.

Acknowledgements

This work was financially supported by National Basic Research Program of China (973 Program) (2014CB931804), the National Natural Science Foundation of China (51473154) and

Fundamental Research Funds for the Central Universities (WK2320000032).

References

1 B. K. Kandola, A. R. Horrocks, P. Myler and D. Blair, *Composites, Part A*, 2002, **33**, 805–817.
2 Z. Bai, L. Song, Y. Hu and R. K. K. Yuen, *Ind. Eng. Chem. Res.*, 2013, **52**, 12855–12864.
3 D. H. Builes and A. Tercjak, *RSC Adv.*, 2015, **5**, 96170–96180.
4 M. C. S. Ribeiro, S. P. B. Sousa, P. R. O. Nóvoa, C. M. Pereira and A. J. M. Ferreira, *IOP Conf. Ser.: Mater. Sci. Eng.*, 2014, **58**, 012020.
5 Z. Bai, L. Song, Y. Hu, X. Gong and R. K. K. Yuen, *J. Anal. Appl. Pyrolysis*, 2014, **105**, 317–326.
6 C. Zhang, J. Y. Huang, S. M. Liu and J. Q. Zhao, *Polym. Adv. Technol.*, 2011, **22**, 1768–1777.
7 M. Sacristán, T. R. Hull, A. A. Stec, J. C. Ronda, M. Galià and V. Cádiz, *Polym. Degrad. Stab.*, 2010, **95**, 1269–1274.
8 K. Dai, L. Song, R. K. K. Yuen, S. Jiang, H. Pan and Y. Hu, *Ind. Eng. Chem. Res.*, 2012, **51**, 15918–15926.
9 R. M. Perez, J. K. W. Sandler, V. Altstädt, T. Hoffmann, D. Pospiech, M. Ciesielski and M. Döring, *J. Mater. Sci.*, 2006, **41**, 341–353.
10 S. Lu and I. Harmerton, *Prog. Polym. Sci.*, 2002, **27**, 1661–1712.
11 M. Spontón, J. C. Ronda, M. Galià and V. Cádiz, *Polym. Degrad. Stab.*, 2008, **93**, 2158–2165.
12 J. W. Gu, G. C. Zhang, S. L. Dong, Q. Y. Zhang and J. Kong, *Surf. Coat. Technol.*, 2007, **201**, 7835–7841.
13 L. L. Pan, G. Y. Li, Y. C. Su and J. S. Lian, *Polym. Degrad. Stab.*, 2012, **97**, 1801–1806.
14 K. Dai, L. Song and Y. Hu, *High Perform. Polym.*, 2013, **25**, 938–946.
15 Q. Wu, J. Lü and B. Qu, *Polym. Int.*, 2003, **52**, 1326–1331.
16 U. Braun, A. I. Balabanovich, B. Schartel, U. Knoll, J. Artner, M. Ciesielski, M. Döring, R. Perez, J. K. W. Sandler, V. Altstädt, T. Hoffmann and D. Pospiech, *Polymer*, 2006, **47**, 8495–8508.
17 M. Xu, W. Zhao and B. Li, *J. Appl. Polym. Sci.*, 2014, **131**, 41159.
18 Y. Li, H. Zheng, M. Xu, B. Li and T. Lai, *J. Appl. Polym. Sci.*, 2015, **132**, 42765.
19 M.-J. Chen, C.-R. Chen, Y. Tan, J.-Q. Huang, X.-L. Wang, L. Chen and Y.-Z. Wang, *Ind. Eng. Chem. Res.*, 2014, **53**, 1160–1171.
20 Z. Tan, C. Wu, M. Zhang, W. Lv, J. Qiu and C. Liu, *RSC Adv.*, 2014, **4**, 41705–41713.
21 L. J. Higham, M. K. Whittlesey and P. T. Wood, *Dalton Trans.*, 2004, 4202–4208, DOI: 10.1039/b411701h.
22 X. Wang, Y. Hu, L. Song, W. Xing, H. Lu, P. Lv and G. Jie, *Polymer*, 2010, **51**, 2435–2445.
23 T. Rajkumar, C. T. Vijayakumar, P. Sivasamy and C. A. Wilkie, *Eur. Polym. J.*, 2008, **44**, 1865–1873.
24 X. Chen, J. Zhuo and C. Jiao, *Polym. Degrad. Stab.*, 2012, **97**, 2143–2147.
25 E. Wawrzyn, B. Schartel, H. Seefeldt, A. Karrasch and C. Jäger, *Ind. Eng. Chem. Res.*, 2012, **51**, 1244–1255.
26 L. Tibiletti, C. Longuet, L. Ferry, P. Coutelen, A. Mas, J.-J. Robin and J.-M. Lopez-Cuesta, *Polym. Degrad. Stab.*, 2011, **96**, 67–75.
27 E. Kandare, B. K. Kandola, D. Price, S. Nazare and R. A. Horrocks, *Polym. Degrad. Stab.*, 2008, **93**, 1996–2006.
28 K. Dai, L. Song, S. Jiang, B. Yu, W. Yang, R. K. K. Yuen and Y. Hu, *Polym. Degrad. Stab.*, 2013, **98**, 2033–2040.
29 M. Bugajny, S. Bourbigot, M. B. Le and R. Delobel, *Polym. Int.*, 1999, **48**, 264–270.
30 Z. Bai, S. Jiang, G. Tang, Y. Hu, L. Song and R. K. K. Yuen, *Polym. Adv. Technol.*, 2014, **25**, 223–232.
31 Y. Zhang, X. Li, Z. Cao, Z. Fang, T. R. Hull and A. A. Stec, *Ind. Eng. Chem. Res.*, 2015, **54**, 3247–3256.
32 G. You, Z. Cheng, Y. Tang and H. He, *Ind. Eng. Chem. Res.*, 2015, **54**, 7309–7319.
33 S. Nazare, B. K. Kandola and A. R. Horrocks, *Polym. Adv. Technol.*, 2006, **17**, 294–303.
34 S. Nazare, B. K. Kandola and A. R. Horrocks, *J. Fire Sci.*, 2008, **26**, 215–242.
35 C. M. C. Pereira, M. Herrero, F. M. Labajos, A. T. Marques and V. Rives, *Polym. Degrad. Stab.*, 2009, **94**, 939–946.
36 Y. Yu, S. Jiang and F. Sun, *Ind. Eng. Chem. Res.*, 2014, **53**, 16135–16142.
37 Q. Tai, Y. Hu, R. K. K. Yuen, L. Song and H. Lu, *J. Mater. Chem.*, 2011, **21**, 6621.
38 A. Fina, H. C. L. Abbenhuis, D. Tabuani and G. Camino, *Polym. Degrad. Stab.*, 2006, **91**, 2275–2281.
39 X. Wang, S. Zhou, W. Xing, B. Yu, X. Feng, L. Song and Y. Hu, *J. Mater. Chem. A*, 2013, **1**, 4383.
40 Z. Bai, X. Wang, G. Tang, L. Song, Y. Hu and R. K. K. Yuen, *Thermochim. Acta*, 2013, **565**, 17–26.
41 Q. Wu and B. Qu, *Polym. Degrad. Stab.*, 2001, **74**, 255–261.
42 S.-H. Liao, P.-L. Liu, M.-C. Hsiao, C.-C. Teng, C.-A. Wang, M.-D. Ger and C.-L. Chiang, *Ind. Eng. Chem. Res.*, 2012, **51**, 4573–4581.

